Advances in Environmental Research, *Vol. 5, No. 1 (2016) 1-18*
DOI: http://dx.doi.org/10.12989/aer.2016.5.1.001

Alanine and serine functionalized magnetic nano-based particles for sorption of Nd(III) and Yb(III)

Ahmed A. Galhoum[1,2], Mohammad G. Mahfouz[2], Asem A. Atia[3], Nabawia A. Gomaa[2], Sayed T. Abdel-Rehem[4], Thierry Vincent[1] and Eric Guibal[*1]

[1]*Centre des Matériaux des Mines d'Alès, Ecole des mines d'Alès, 6 avenue de Clavières, F-301319 Alès cedex, France*
[2]*Nuclear Materials Authority, P.O. Box 530, El-Maadi, Cairo, Egypt*
[3]*Chemistry Department, Faculty of Science, Menoufia University, Shebin El-Kom, Egypt*
[4]*Chemistry Department, Faculty of Science, Ain Shams University, Ain Shams, Egypt*

(Received July 23, 2015, Revised January 4, 2016, Accepted January 15, 2016)

Abstract. Magnetic nano-based sorbents have been synthesized for the recovery of two rare earth elements (REE: Nd(III) and Yb(III)). The magnetic nano-based particles are synthesized by a one-pot hydrothermal procedure involving co-precipitation under thermal conditions of Fe(III) and Fe(II) salts in the presence of chitosan. The composite magnetic/chitosan material is crosslinked with epichlorohydrin and modified by grafting alanine and serine amine-acids. These materials are tested for the binding of Nd(III) (light REE) and Yb(III) (heavy REE) through the study of pH effect, sorption isotherms, uptake kinetics, metal desorption and sorbent recycling. Sorption isotherms are well fitted by the Langmuir equation: the maximum sorption capacities range between 9 and 18 mg REE g^{-1} (at pH 5). The sorption mechanism is endothermic (positive value of $\Delta H°$) and contributes to increase the randomness of the system (positive value of $\Delta S°$). The fast uptake kinetics can be described by the pseudo-second order rate equation: the equilibrium is reached within 4 hours of contact. The sub-micron size of sorbent particles strongly reduces the contribution of resistance to intraparticle diffusion in the control of uptake kinetics. Metal desorption using acidified thiourea solutions allows maintaining sorption efficiency for at least four successive cycles with limited loss in sorption capacity.

Keywords: rare-earth element; magnetic sorbent; nano-based particles; neodymium; ytterbium; amino-acid functionalized chitosan; sorption isotherms; uptake kinetics; thermodynamics; metal desorption; sorbent recycling

1. Introduction

The use of rare earth elements (REEs) is widespread in industry due to the increasing demand for developing photo-electronic products, but also for nuclear sector (radiation detector, plutonium "diluent", structural materials and flux controller). On the other hand, the resource for the production of these metals is distributed in a limited number of countries and China has a quasi-monopole in the commercial production of this important resource necessary to the manufacturing

*Corresponding author, Ph.D., E-mail: eric.guibal@mines-ales.fr

http://www.techno-press.org/?journal=aer&subpage=7 ISSN: 2234-1722 (Print), 2234-1730 (Online)

of high-tech equipment. For these reasons, the recovery of REEs from non-conventional resources such as sub-products of other mineral resources (phosphate rocks, uranium mining) or from urban mining (recycling and valorization of waste electrical and electronic equipment, WEEEs) is becoming a strategic issue for relevant industry (Xu and Peng 2009, Innocenzi *et al*. 2014). Another rationale consists in the drastically increasing regulations concerning the recycling of waste materials; for example the WEEE directive from the European Community fixes objectives for the valorization and recycling of spent electronic and electrical devices.

Conventional processes in the treatment of dilute effluents are frequently limited by technical causes, environmental constraints or economic reasons. For example, precipitation is generally non-selective, and produces huge amount of contaminated solid wastes. Solvent extraction processes are well known and efficient for the treatment of concentrated solutions (Vander Hoogerstraete and Binnemans 2014, Xie *et al*. 2014), but fail to achieve competitive recovery for low-concentration effluents. A concentrating process is thus preferred consisting in sorption processes using ion-exchange or chelating resins, sorbents (more or less complex) (Wang *et al*. 2002, Sun *et al*. 2009, Abdel-Rahman *et al*. 2010), prior to proceed to solvent extraction and/or electrochemical processes. The competitiveness of sorption processes depends on the concentration of the metal, the complexity of the solution, the target objective (complete recovery, separation performance), and the cost of the sorbent. As an alternative to conventional resins, some biopolymers have been deeply investigated for the recovery of metal ions from dilute solutions. Chitosan (an aminopolysaccharide constituted of D-glucosamine and N-acetyl-D-glucosamine units) is a good illustration of the potential offered by renewable marine resources for metal binding (environmental and valorization aspects). This biopolymer can bind metal cations by chelation on the free electron doublets of nitrogen (on free amine groups) at near-neutral pH, or by ion-exchange/electrostatic attraction mechanism for metal anions in acidic solutions (Guibal 2004). The functional groups present on the polymer backbone (i.e., hydroxyl and amine groups) make this material readily modifiable by chemical grafting (Khan *et al*. 2011). It is thus possible immobilizing on chitosan different groups to increase the density of reactive groups, to improve the selectivity or enhance the pH range for optimal use. These reactive groups may be sulfur, amine or carboxylic functions, or amino-acids (Oshita *et al*. 2007, Hosoba *et al*. 2009).

The sorption properties of chitosan are limited by two potential drawbacks (depending on the metal and the optimal pH): the stability of the biopolymer in acidic solutions and the poor porosity of the raw material. For preventing chitosan dissolving in acidic solutions it may be necessary crosslinking the biopolymer (Zhou *et al*. 2010); however, this crosslinking should orientated to prevent the reactive amine groups to be involved. The poor porosity of chitosan induces diffusion limitations that can be minimized by decreasing the size of sorbent particles (at the expense of difficulties in recovering spent materials at the end of the process or limitations in the use of these materials in fixed-bed columns with high head pressure loss and clogging effects) or synthesizing conditioned materials (such as gel beads, membranes and foams, etc.) (Ruiz *et al*. 2002a, b).

The sorbents used in this study have been previously elaborated for the sorption of dysprosium (Galhoum *et al*. 2015). For minimizing diffusion limitations and slow kinetics, the process preferred for the synthesis of these materials consisted in using micron-size particles combining a magnetic core and a coating with functionalized chitosan. Amino-acids have been grafted on chitosan backbone through epichlorohydrin crosslinking. These particles are associating the reactivity of chitosan (direct sorption and readily chemical modification), the fast kinetics of nano-based particles and the easy recovery of spent material particles by external magnetic field. Incorporating magnetic nanoparticles in sorbents has already been documented (Donia *et al*. 2007,

Wu *et al*. 2011); these materials show promising perspectives for applications in environmental and health fields (Ren *et al*. 2013, Xu *et al*. 2013, Yang *et al*. 2014, Zhou *et al*. 2014). After investigating the effect of pH on Nd(III) (a light REE) and Yb(III) (a heavy REE), uptake kinetics have been compared for the two sorbents. The effect of the temperature on sorption isotherm was also considered for determining the thermodynamic parameters. Metal desorption and sorbent recycling were also investigated.

2. Materials & methods

2.1 Materials

The synthesis of sorbents was previously described (Galhoum *et al*. 2015). This is based on a series of successive steps consisting in: (a) synthesis of magnetic/chitosan nano-based particles (hydrothermal precipitation of iron salt precursors in the presence of chitosan, (b) crosslinking of chitosan with epichlorohydrin, and (c) grafting of amino-acids (through epichlorohydrin-based linkage).

Basically, the magnetic-chitosan nano-based particles were obtained by dissolving and mixing chitosan (in acetic acid solution) with Fe(III) and Fe(II) salts (molar ratio 1:2 between iron(II) sulfate and iron(III) chloride salts) before increasing the pH to 10 under heating (with reflux). Black nano-based particles were then crosslinked with epichlorohydrin to stabilize chitosan in a wider pH range. Finally, amino acids were grafted, by (i) mixing cross-linked particles with epichlorohydrin in a mixture of ethanol and water (1:1 v/v) under reflux, before (ii) separating the functionalized nano-based particles and washing out the residues of reagents with alcohol and water, and (iii) reacting the intermediary product with amino-acids dissolved in dioxane under reflux. After alternate washing with ethanol and water the materials were freeze-dried. The proposed structures of synthesized derivatives of chitosan are presented in Fig. 1; Fig. AM1, in the Additional Material Section, shows the detailed procedure for the synthesis of alanine functionalized chitosan nano-based particles (similar process occurs with serine grafting on magnetic chitosan nano-based particles).

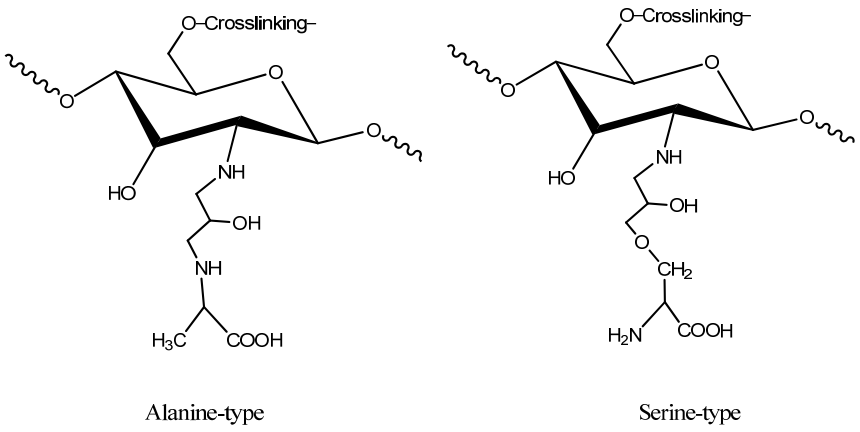

Alanine-type Serine-type

Fig. 1 Structure of alanine and serine functionalized chitosan materials

2.2 Sorption process

REE chloride salts ($NdCl_3.xH_2O$ and $YbCl_3.xH_2O$) were purchased from Sigma-Aldrich and were burned off at 900°C for 3 h. Stock solutions of REE(III) were prepared by dissolving the burnt salts in concentrated sulfuric acid under heating before being diluted with demineralized water until final concentration of 1000 mg REE L^{-1}. The working solutions were prepared by appropriate dilution of the stock solutions immediately prior to use. The metal concentrations in both initial and processed samples were determined by an Inductively Coupled Plasma Atomic Emission Spectrometer (ICP-AES JY Activa M, Jobin-Yvon, Longjumeau, France).

Batch experiments were carried out by contact of 20 mg of sorbent with 100 mL of aqueous metal ion solution (100 mg REE(III) L^{-1}) at fixed initial pH in polypropylene centrifuge tube, under agitation (300 rpm) and at 300 K for 4 hours. After equilibration and phase separation, the pH was recorded and the residual metal concentration in the aqueous phase was estimated by ICP-AES, whilst the concentration of metal ions sorbed onto the functionalized chitosan was obtained by the mass balance equation, Eq. (1)

$$q = \frac{\left(C_0 - C_{eq}\right) \times V}{m} \tag{1}$$

Here q is the amount of sorbed metal ions (mg REE g^{-1} sorbent), while C_0 and C_{eq} are the initial and equilibrium metal ion concentrations (mg REE L^{-1}) in the aqueous solution, respectively. V is the volume of the solution (0.02 L) and m is the mass of the sorbent (0.05 g).

For the study of sorption properties several parameters were successively investigated: the influence of pH, uptake kinetics, sorption isotherm (including the influence of temperature), metal desorption and sorbent recycling. Isotherm studies were investigated by mixing a fixed amount of sorbent (i.e., 0.05 g) with 20 mL of REE(III) solution at different initial concentrations (i.e., 25, 50, 75, 100, 150, 200 and 300 mg L^{-1}, at pH 5) and shaking for 4 h at 300 rpm. The experiments were performed in a thermostatic chamber, at different temperatures (300±1 K, 310±1 K and 320±1 K, respectively). Uptake kinetics was performed using a sorbent dosage of 2.5 g L^{-1} and a concentration of 100 mg REE L^{-1} at 300±1 K: samples were collected under agitation at standard times and metal concentration was determined, after magnetic separation, by ICP-AES. Main experimental conditions have been summarized in the caption of the figures.

Thiourea (0.5 M) solution acidified (to pH 2.5-3) with few drops of H_2SO_4 (0.2 M) was chosen as the eluant for the study of metal desorption. The contact time between the eluent and the metal-loaded sorbent was set to 1 h (under constant agitation). The sorption yield after regeneration for four cycles was compared to the value reached for the first cycle.

2.3 Brief reminder on the characteristics of the sorbents

These materials (alanine and serine functionalized chitosan magnetic nano-based particles) were previously tested for the sorption of Dy(III) and they were carefully characterized using a series of analytical techniques such as Fourier-transform infra-red spectrometry (FTIR), X-ray diffraction (XRD) and elemental analysis, vibrating sample magnetometry (VSM), and transmission electron microscopy (TEM) (Galhoum *et al*. 2015). The XRD patterns presented a series of characteristic peaks that can be directly assigned to Fe_3O_4 (i.e., an iron oxide material having a spinel structure with interesting magnetic properties); the Debye-Scherrer equation was used to approach the size of nano-crystals (i.e., 13.0 and 11.6 nm for alanine- and serine-based

sorbents, respectively). The magnetic behavior of sorbent particles was determined by VSM: 10.6 and 14.0 emu g^{-1} for alanine- and serine-based sorbents, respectively. The absence of remanence and coercivity on magnetization loops confirmed the superparamagnetic properties of the sorbents and their potential for magnetic separation; though their saturation magnetization was much lower than expected values for pure magnetite. TEM observations confirmed the nanometer-size of sorbent particles (roughly spherical), though natural magnetic attraction leaded to self-aggregation of particles that form aggregates of 15-40 nm in size. In addition, TEM images showed a dark central part corresponding to magnetic core, coated with a translucent surrounding zone (corresponding to functionalized chitosan layer). Weight loss of sorbents at 600°C showed that about 50 % of total mass is mineral (made of iron oxide). Both elemental analysis and FTIR characterization confirmed the changes in the content of nitrogen/amine groups in the material at the different stages of the synthesis: the grafting of amino-acids on the chitosan was demonstrated by (a) the increase of nitrogen mass percentage (elemental analysis), and the intensity of amine and amide peaks (FTIR spectrometry), but also (b) the appearance of carboxylate groups on FTIR spectra. The peaks relevant to crosslinking procedure were also identified in the intermediary steps of the synthesis and progressively disappeared after amino-acid grafting. FTIR spectra also confirmed the presence of Fe_3O_4 (characterized by the presence of the Fe-O stretching band).

3. Results & discussion

3.1 pH effect on metal sorption

The pH may impact the surface properties of sorbent (protonation/deprotonation of reactive groups) and the speciation of metal species (formation of hydrolysed species or complexes). In the case of REE metal ions in simple solutions (without additional ligands) the speciation is not substantially changed and most of the effect of pH will proceed through the change of the overall charge of the sorbent and more specifically on the deprotonation of amine and carboxylate groups. Metal ions are present under the form of Nd^{3+} and Yb^{3+} in acidic solutions and tend to form cationic hydrolyzed species (such as $Nd(OH)^{2+}$, $Nd(OH)_2^{+}$ or $Yb(OH)^{2+}$, $Yb(OH)_2^{+}$) when increasing the pH. At higher pH (i.e., above pH 6) species such as $Nd(OH)_3$, and $Yb(OH)_3$ may appear; and at high concentration metal ions begin to precipitate. As a consequence, in slightly acidic solutions cationic metal species may co-exist under different forms (depending on pH and metal concentration). On the other hand amine groups of chitosan have a pK_a close to 6.5, while the pK_a*s* for alanine and serine are 2.33 and 2.21 (carboxyl groups) and 9.71 and 9.12 (for amine groups), respectively. Though the acid base properties may be significantly affected by chemical grafting and change in the chemical environment of reactive groups this means that in acidic solutions (pH below 2) the sorbents will be fully protonated, while at slightly acidic pH (i.e., around pH 5) will co-exist carboxylate groups and free amine groups (deprotonated), which both are able to interact with metal cations through either chelation or electrostatic attraction. Fig. 2 shows that the sorption of both Nd(III) and Yb(III) increases with increasing the pH for both alanine-based and serine-based sorbents. The sorption capacity slightly increases between pH 1 and pH 3-4 and sharply increases above pH 4 before tending to stabilize above pH 5. These results are consistent with previous comments on the chemistry of reactive groups and metal species.

Fig. 2 also shows the change in the pH during metal sorption: between pH 1 and 2 the pH hardly varies while a strong increase in the pH is observed when initial pH raises to 3 the

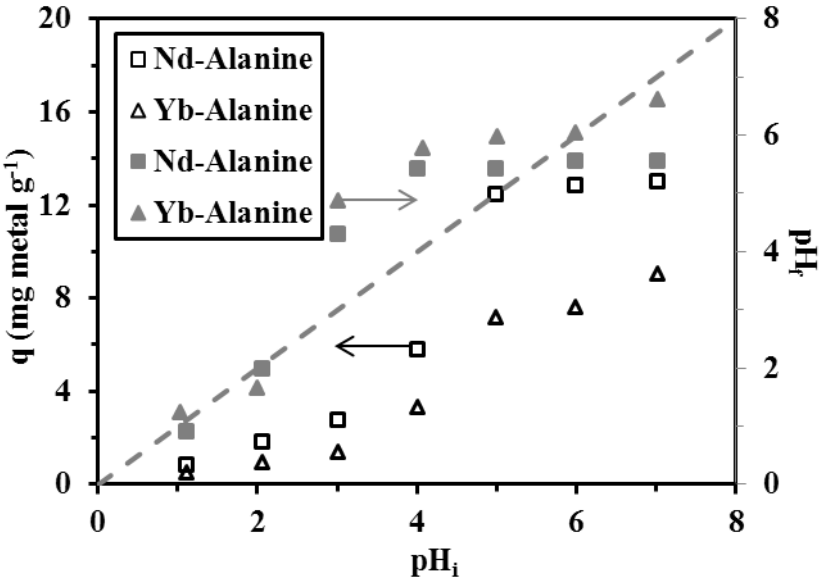

Fig. 2 Effect of initial pH on sorption capacity (open symbols) and equilibrium pH (closed symbols) for the recovery of Nd(III) and Yb(III) using alanine and serine functionalized chitosan magnetic nano-based particles (C_0: 100 mg metal L^{-1}; sorbent dosage, SD: 2.5 g L^{-1}; contact time: 4 h; T: 20°C)

equilibrium pH stabilizes between 4.5 and 5. At initial pH above 4 the equilibrium pH tends to stabilize between pH 5.5 and 6. There is clear correlation between the increase in the pH of the solution and the increase in the sorption capacity. Intermediary pH (i.e., in the range 4.5-5) allows maintaining the reactive groups at the surface of the sorbents under deprotonated forms (carboxylate and free amine groups) favorable to the sorption of cationic REE species. It is noteworthy that it is necessary selecting a pH higher than 2 to prevent partial dissolving of magnetic core and lower than 6 to prevent metal precipitation at metal concentration higher than 100-150 mg L^{-1}. For example in the case of Yb(III) sorption, the slight increase of sorption capacity observed at pH 7 is probably associated to metal precipitation. For these reasons, taking into account optimum efficiency, pH variation and both the stability of the sorbent and the speciation of metal ions, further experiments were performed at initial pH 5.

3.2 Uptake kinetics

Uptake kinetics is critical for the design of the sorption process. The rationale of synthesizing magnetic nano-based sorbents consists in reducing the contribution of resistance to intraparticle diffusion to the control of uptake kinetics (together with a readily recovery). Indeed, kinetic profiles are generally controlled by a series of mechanisms of resistance, including bulk diffusion, film diffusion and intraparticle diffusion. An efficient mixing power is generally sufficient for limiting the impact of bulk diffusion, reducing the size of sorption particles limits the effects of film diffusion and intraparticle diffusion. Fig. 3 compares the kinetic profiles for the sorption of Nd(III) and Yb(III) with both alanine and serine functionalized magnetic nano-based particles: sorption capacity is plotted as a function of time. Actually, all the curves show three sections:

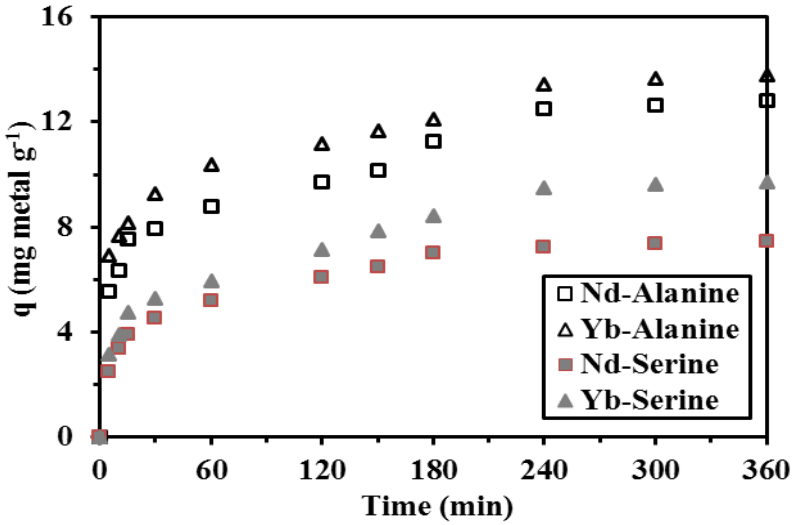

Fig. 3 Uptake kinetics for the recovery of Nd(III) and Yb(III) using alanine and serine functionalized chitosan magnetic nano-based particles (C_0: 100 mg metal L^{-1}; sorbent dosage, SD: 2.5 g L^{-1}; pH_i: 5; *T*: 20°C)

(a) 0-20 min: a strong increase in sorption capacity (steep initial slope that reflects a significant decrease in the relative concentration of the metal ions in the solution): this corresponds to the fast sorption of metal ions on the reactive groups located at the external surface of the sorbent particles (coupled to the effect of film diffusion, which is usually active in the first minutes of contact). This steps corresponds to 60-70 % of total sorption for all the systems (sorbent/metal)

(b) 20 min-4 h: a progressive increase in sorption capacity (with a lower slope) that corresponds to the progressive saturation of reactive groups in the biopolymer layer covering the magnetic core. This may be controlled by the resistance to intraparticle diffusion (and to the swelling of this biopolymer layer).

(c) 4 h-6 h: a very slow sorption phase that counts for a few percent of the total sorption capacity: this is associated to the full saturation of internal groups and to a small extent to the sorption on magnetic core of the sorbent.

Uptake kinetics can be modeled using a number of models that may combine film diffusion, intraparticle diffusion, reaction rate (Tien 1994). These models require a perfect characterization of sorbent particles and complex mathematical resolutions. Alternative and simpler models are also frequently used for modeling kinetic profiles, such as the pseudo-first order rate equation (PFORE), the pseudo-second order rate equation (PSORE), the Elovich equation or the simplified resistance to intraparticle diffusion equation (sRIDE) (Table 1). PFORE and PSORE equations have been initially developed for modeling chemical reactions in homogeneous systems before being extended to heterogeneous systems. However, this transfer to heterogeneous systems means that the parameters of these models should be considered as apparent parameters that implicitly integrate the contribution of diffusion resistance (especially resistance to intraparticle diffusion). The four equations reported in Table 1 have been tested for modeling experimental data reported in Fig. 3. Tables 2 and 3 summarize the values of the parameters of these models (together with their relevant correlation coefficient). Figs. AM2-AM5 (see Additional Material Section) shows the plots of kinetic profiles using the linearized forms the different models. Both the curves and

the correlation coefficients reported in Tables 2-3 confirm that the PSORE fits better experimental data than the other models.

The best fit of experimental data with the PSORE (compared to the PFORE) is also confirmed by the good correlation of the values of sorption capacity at equilibrium for calculated (simulated) data ($q_{eq,1}$ or $q_{eq,2}$) and experimental data ($q_{eq,exp}$), while substantial differences were observed when using the PFORE. In the case of alanine-based sorbent, the apparent kinetic parameter (k_2) was not affected by the metal (3.5×10^{-3} vs. 3.1×10^{-3} mg g^{-1} min^{-1} for Nd(III) and Yb(III), respectively). In the case of serine-based sorbent Nd(III) appears to be fast sorbed compared with Yb(III): the kinetic coefficient decreased from 6.3×10^{-3} mg $g^{-1}min^{-1}$ for Nd(III) to 3.4×10^{-3} mg g^{-1} min^{-1} for Yb(III). Similarly alanine-based and serine-based sorbents have comparable kinetic coefficients for Yb(III) around $3.1\text{-}3.4\times10^{-3}$ mg g^{-1} min^{-1} while in the case of Nd(III) serine-based sorbent was faster than alanine-based sorbent. This could be explained by the easier accessibility of reactive groups on serine-based material (amine groups and carboxylate groups being available at the end of the grafted chain, while for alanine-based sorbent only carboxylate groups are directly accessible).

The modeling of kinetic profiles with the simplified model of resistance to intraparticle diffusion fails to fit experimental data. While a single linear plot is expected for verifying the contribution of intraparticle diffusion in the control of uptake kinetics, in some cases (corresponding to different steps associated to different sizes of porous networks) the plot can be simulated by several successive linear sections. In the present case the curvature of the fits does

Table 1 Kinetic models: equations and linearized forms

	Equation	Linearized form
Pseudo-first order rate equation (PFORE) (Lagergren 1898)	$q(t) = q_{eq,1}\,[1 - e^{-k_1 t}]$	$\log(q_{eq,1} - q(t)) = \log q_{eq,1} - \left(\frac{k_1}{2.303}\right) t$
Pseudo-second order rate equation (PFORE) (Ho and McKay 1999)	$q(t) = \frac{k_2\, q_{eq,2}^2\, t}{1 + k_2\, q_{eq,2}\, t}$	$\frac{t}{q(t)} = \frac{1}{k_2 q_{eq,2}^2} + \left(\frac{1}{q_{eq,2}}\right) t$
Elovich equation (Zeldowitsch 1934)	-	$q(t) = A_E + B_E \ln t$
Simplified resistance to intraparticle diffusion equation (sRIDE) (Weber and Morris 1963)	-	$q(t) = K_{int} t^{0.5} + C$

Table 2 Modeling of uptake kinetics with the PFORE and PSORE equations for Nd(III) and Yb(III) recovery using alanine and serine functionalized chitosan magnetic nano-based particles

Sorbent	Metal ion		PFORE				PSORE		
		$q_{eq,exp}$ (mg g^{-1})	$q_{eq,1}$ (mg g^{-1})	$k_1\times10^3$ (min^{-1})	R^2	$q_{eq,2}$ (mg g^{-1})	$k_2\times10^3$ (mg g^{-1} min^{-1})	R^2
Alanine	Nd(III)	12.8	6.4	8.1	0.939	13.2	3.5	0.988
	Yb(III)	13.8	5.9	8.2	0.976	14.1	3.1	0.994
Serine	Nd(III)	7.5	2.0	6.8	0.927	7.77	6.3	0.996
	Yb(III)	9.7	2.3	4.2	0.939	10.2	3.4	0.987

Table 3 Modeling of uptake kinetics with the sRIDE and the Elovich equations for Nd(III) and Yb(III) recovery using alanine and serine functionalized chitosan magnetic nano-based particles

Sorbent / Metal ion		sRIDE			Elovich		
		C (mg g^{-1})	K_{int} (mg g^{-1} $min^{-0.5}$)	R^2	B_E (J mol^{-1})	A_T (L g^{-1})	R^2
Alanine	Nd(III)	3.82	0.54	0.853	1.69	2.46	0.952
	Yb(III)	4.79	0.55	0.801	1.65	3.83	0.977
Serine	Nd(III)	1.91	0.34	0.884	1.19	0.56	0.993
	Yb(III)	2.07	0.45	0.927	1.58	0.22	0.965

not show any linear sections and the curves do not pass through the origin (See Fig. AM5, in Additional Material Section). This is a confirmation that this model is not appropriate for describing the sorption kinetics (correlation coefficients in Table 3 confirm this conclusion). This is consistent with the objective of reducing the size of sorbent particles to reduce the limiting effect of resistance to intraparticle diffusion. Better fits of experimental data were obtained using the Elovich model (correlation coefficients ranging between 0.952 and up to 0.993). However, the Elovich plot fails to linearly fit experimental data at large contact time (i.e., above 120 min); this means that at the approach of equilibrium the model is not appropriate.

These results confirm that reducing the size of sorbent particles allows reducing the contribution of the resistance to intraparticle diffusion: a contact time of 4 hours is sufficient for reaching the equilibrium and the kinetic profiles can be modeled using the pseudo second order rate equation (PSORE).

3.3 Sorption isotherms and thermodynamics

Sorption isotherms plot the distribution of the solute between the liquid and solid phases at equilibrium; this is represented by the function $q=f(C_{eq})$. The sorption isotherms have been carried out at different temperatures for both Nd(III) and Yb(III) using alanine-based sorbent (Fig. 4) and serine-based sorbent (Fig. 5), in order to evaluate the thermodynamic parameters.

All the curves are characterized by a similar shape: (a) a first initial steep slope (at low residual concentration), followed by (b) a progressive increase in sorption capacity (corresponding to a residual increase of about 150 mg metal L^{-1}) and (c) a saturation plateau.

Maximum sorption capacities range between 14 and 16 mg Nd g^{-1}, and between 16 and 18 mg Yb g^{-1} for alanine-based sorbents and the sorption capacity increases with temperature: the sorption is endothermic. Similar trend is observed for serine-based sorbent: sorption capacities increase with temperature from 8 to 10 mg Nd(III) g^{-1} and from 9 to 11 Yb(III) g^{-1}. These maximum sorption capacities are comparable to the values reached with *Saccharomyces cerevisiae* for Nd(III), i.e., 10-20 mg Nd g^{-1} (Vlachou *et al*. 2009), *Pseudomonas aeruginosa*, i.e., 24 mg Yb g^{-1} (Texier *et al*. 1999) or *Turbinaria conoides*, i.e., 34 mg Yb g^{-1} (Vijayaraghavan *et al*. 2011). In the case of Nd(III) the sorption capacity of chitosan does not exceed 4 mg Nd g^{-1} but increases to 70 mg Nd g^{-1} when EDTA or DTPA are grafted onto chitosan backbone (Roosen and Binnemans 2014). The grafting of phonic groups onto silica microparticles allowed obtaining sorbents with sorption capacities close to 40 mg Nd g^{-1} (Melnyk *et al*. 2012). The same order of magnitude (i.e., 48 mg Nd g^{-1}) was obtained in the case of Levextrel resins impregnated with trialkylphosphine

oxide (Zhang *et al*. 2012). These performances are generally much lower than the sorption levels reached with specific resins: about 266 mg Yb g^{-1} and 308 mg Nd(III) g^{-1} for a gel type weak acid

Table 4 Sorption isotherm models: equations and linearized forms

	Equation	Linearized form
Langmuir (Langmuir 1918)	$q_{eq} = \frac{q_{\max} b C_{eq}}{1 + b C_{eq}}$	$\frac{C_{eq}}{q_{eq}} = \frac{C_{eq}}{q_{\max}} + \frac{1}{q_{\max} \times b}$
Freundlich (Freundlich 1906)	$q_{eq} = K_F C^{1/n}$	$\ln(q_{eq}) = \ln(K_F) + \frac{1}{n}\ln(C_{eq})$

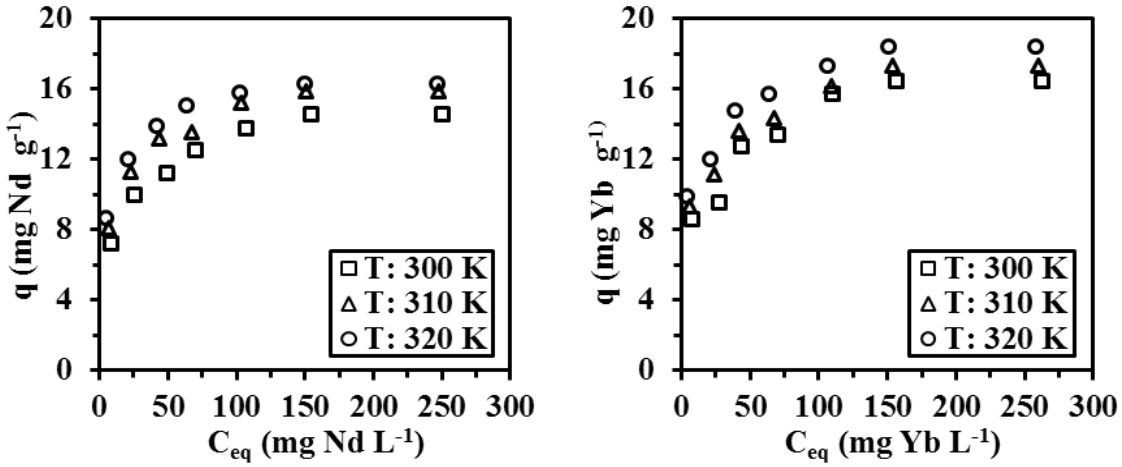

(a) Nd(III) (b) Yb(III)

Fig. 4 Sorption isotherms at different temperatures for the recovery of Nd(III) and Yb(III) using alanine functionalized chitosan magnetic nano-based particles (pH_i 5)

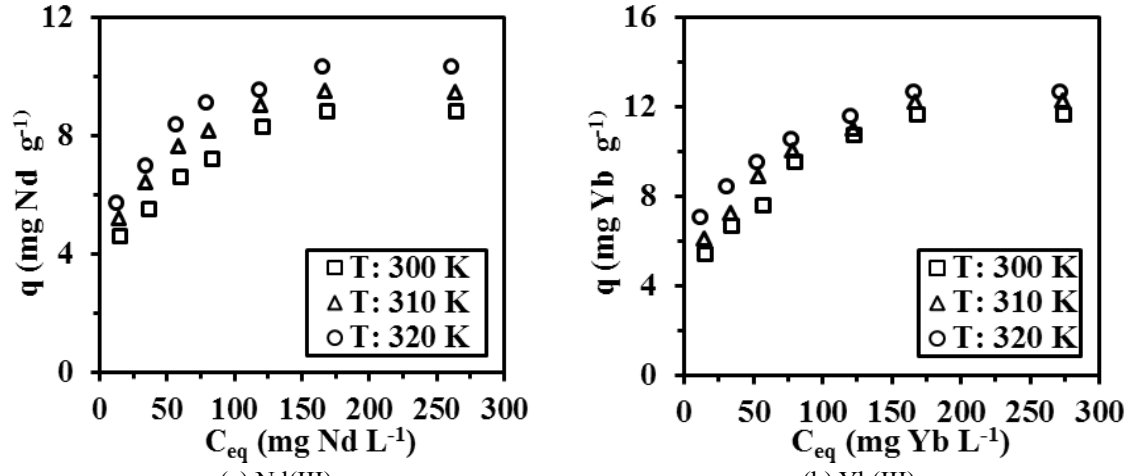

(a) Nd(III) (b) Yb(III)

Fig. 5 Sorption isotherms at different temperatures for the recovery of Nd(III) and Yb(III) using serine functionalized chitosan magnetic nano-based particles (pH_i 5)

Table 5 Modeling of sorption isotherms with the Langmuir and the Freundlich equations for the recovery of Nd(III) and Yb(III) using alanine and serine functionalized chitosan magnetic nano-based particles

Sorbent / Metal ion		T (K)	$q_{eq,exp}$ (mg g^{-1})	Langmuir q_{max} (mg g^{-1})	Langmuir b (L mg^{-1})	Langmuir R^2	Freundlich K_F	Freundlich 1/n	Freundlich R^2
Alanine	Nd(III)	300	14.5	15.3	0.085	0.998	0.79	0.217	0.961
		310	15.9	16.5	0.116	0.998	6.06	0.190	0.952
		320	16.3	16.7	0.171	0.999	7.08	0.168	0.940
	Yb(III)	300	16.5	17.4	0.075	0.998	5.40	0.733	0.921
		310	17.3	18.2	0.083	0.998	6.73	0.828	0.966
		320	18.4	19.1	0.108	0.999	7.81	0.893	0.965
Serine	Nd(III)	300	8.9	9.1	0.102	0.977	2.30	0.255	0.964
		310	9.5	9.6	0.188	0.983	3.02	0.220	0.958
		320	10.4	10.5	0.214	0.985	3.50	0.208	0.959
	Yb(III)	300	11.7	12.4	0.057	0.982	2.42	0.297	0.953
		310	12.3	12.8	0.076	0.987	3.13	0.257	0.966
		320	12.7	13.1	0.108	0.989	4.35	0.201	0.979

Table 6 Thermodynamics of Nd(III) and Yb(III) sorption using alanine and serine functionalized chitosan magnetic nano-based particles

Sorbent / Metal ion		T (K)	$\Delta H°$ (kJ mol^{-1})	$\Delta S°$ (J mol^{-1} K^{-1})	$\Delta G°$ (kJ mol^{-1})	$T\Delta S°$ (kJ mol^{-1})	R^2
Alanine	Nd(III)	300	27.76	171	-23.45	53.30	0.993
		310			-25.52	53.01	
		320			-26.86	54.72	
	Yb(III)	300	12.95	122	-23.63	36.60	0.859
		310			-24.85	37.82	
		320			-26.07	39.04	
Serine	Nd(III)	300	29.87	180	-24.12	53.97	0.887
		310			-25.92	55.77	
		320			-27.72	57.57	
	Yb(III)	300	25.79	162	-22.89	48.66	0.994
		310			-24.51	50.28	
		320			-26.13	51.90	

resin (-COOH based resin) (Zheng and Xiong 2011, Xiong *et al*. 2015), or 187 mg Yb g^{-1} with an iminiodiacetic acid resin (Xiong *et al*. 2006).

Sorption isotherms can be described by different models (Table 4): the most frequently used are the Langmuir and the Freundlich equations. These models were initially developed for describing gaz/solid systems before being extended to liquid/solid equilibria. The Langmuir equation assumes the sorption to be uniform in terms of sorption energies (interactions between solute molecules and sorption sites), to occur as a monolayer without interactions between sorbed molecules. On the

other hand, Freundlich equation is an empirical equation associated to possible heterogeneities of the sorbent (with different sorption energies and possible interactions between sorbed molecules).

Table 5 reports the parameters of the two models for the different systems metal/sorbent. The correlation coefficients are systematically higher with the Langmuir model than with the Freundlich equation. This is consistent with the shape of sorption isotherms: the Langmuir equation has an asymptotic trend (indicated by a saturation plateau) contrary to the exponential form of the Freundlich equation. It is noteworthy that not only the maximum sorption capacities but also the affinity coefficient (the parameter b of the Langmuir equation) are increasing with temperature. The Freundlich exponent (1/n) is systematically smaller than 1: this means that the sorption is favorable over the entire range of concentration (a value of 1/n higher than 1 would indicate that the sorption begins to be favorable only at high solute concentration).

The "favorability" of the sorption process can be determined by calculating the coefficient R_L (dimensionless)

$$R_L = \frac{1}{1 + bC_0} \tag{2}$$

where b is the Langmuir constant (L mg^{-1}) and C_0 the initial concentration of metal ions in the solution (mg L^{-1}). The R_L coefficients were calculated for all sorbent/metal systems using an initial concentration of 250 mg metal L^{-1} (corresponding to saturation plateau), 50 mg metal L^{-1} (corresponding to conventional range of metal concentration for sorption processes) and 10 mg metal L^{-1} (corresponding to concentration order for polishing treatment). Systematically, the R_L coefficient ranged between 0.02 and 0.07, between 0.08 and 0.027, and between 0.31 and 0.64 for C_0: 250, 50 and 10 mg metal L^{-1}, respectively. Regardless of the sorbent, the metal and the concentration RL was systematically lower than 1.0: this means that the sorption of Nd(III) and Yb(III) on both alanine-based and serine-based sorbents is favorable.

The thermodynamic parameters of sorption can be obtained by the van't Hoff equation

$$\ln b = \frac{-\Delta H^\circ}{RT} + \frac{\Delta S^\circ}{R} \tag{3}$$

$$\Delta G^\circ = \Delta H^\circ - T\Delta S^\circ \tag{4}$$

The free energy of (ΔG°, kJ mol^{-1}) is systematically negative regardless of the sorbent and tends to decrease with increasing the temperature: the increase in temperature favors the sorption process. The positive value of the enthalpy change (ΔH°, kJ mol^{-1}) confirms the endothermic nature of the sorption process while the positive value of the entropy change (ΔS°) means that the randomness of the global system increases after metal sorption. This may be explained by the release of water of hydration bound to REE metal ions during metal sorption. In addition, the fact that $|\Delta H^\circ| < |T\Delta S^\circ|$ indicates that the sorption process is controlled by entropic rather than enthalpic changes.

3.4 Metal desorption and sorbent recycling

The sorption performance for the recovery of both Nd(III) and Yb(III) using alanine-based and serine-based sorbents was tested over four successive sorption/desorption cycles. Desorption was operated using acidic solutions of thiourea and metal sorption was systemically performed under the same sorption conditions. Table 7 reports the values of the efficiency of metal sorption and the

sorption capacities at the different cycles. The sorption performance progressively decreases: the loss in sorption efficiency and sorption capacity never exceeds 5% at the fourth sorption stage. Metal desorption is feasible and the recycling of the sorbent can be operated for a minimum of 4 cycles.

3.5 Nd(III)/Yb(III) separation

The recovery and valorization of REEs is usually facing several challenges: first the separation of REEs from base metals (when processing phosphate rocks, uranium ores or WEEEs; however, due to very close physicochemical properties within the REE family the most difficult remains the selective separation of REEs when present in multi-component solutions. Neodymium is part of the light REEs while ytterbium is generally considered as a heavy REE: checking the possible separation of these two metals ions from equimolar binary solutions will contribute to establish the possibility to use these sorbents for separation light and heavy REEs. Table 8 reports the molar ratio between Yb(III) and Nd(III) in the different compartments (i.e., molar ratio in the initial solution, and at equilibrium together with the relative molar ratio of the REEs in the sorbent).

It is noteworthy that, basically, the two sorbents show similar trends: Yb(III) preferentially accumulates on the sorbent while Nd(III) concentrates in the solution. However, the values of the molar ratios are not large enough to allow an effective and efficient separation of these metals. This is confirmed by the values of the separation factor, $\alpha_{Yb/Nd}$, which varies around 2 (slightly higher for serine-based sorbent). This means that the selective separation of Yb(III) from Nd(III), cannot be operated in a single stage: it will be necessary using successive compartments to reach a sufficient level of separation (conventional industrial process for the separation of REEs), or using ligands to improve the separation of complexed REEs (Hubicka and Kolodynska 2000).

Table 7 Variation of sorption efficiency for the recovery of Nd(III) and Yb(III) along 4 successive sorption/desorption cycles using alanine and serine functionalized chitosan magnetic nano-based particles

Cycle	Alanine - Nd(III)		Alanine - Yb(III)		Serine - Nd(III)		Serine - Yb(III)	
	q_e (mg Nd g^{-1})	Ads. Eff. (%)	q_e (mg Yb g^{-1})	Ads. Eff. (%)	q_e (mg Nd g^{-1})	Ads. Eff. (%)	q_e (mg Yb g^{-1})	Ads. Eff. (%)
I	12.5	100.0	13.4	100.0	7.2	100.0	9.6	100.0
II	12.3	98.2	13.2	98.1	7.1	98.5	9.4	98.2
III	12.2	97.2	13.0	97.0	7.1	97.4	9.3	97.7
IV	12.1	96.6	13.0	96.4	7.0	96.8	9.3	97.1

Table 8 Separation of Nd(III) and Yb(III) from binary solutions ([Yb(III)/Nd(III)] molar ratio in the solution at t=0, at equilibrium, and in the sorbent; selectivity coefficient $\alpha_{Yb/Nd}$)

	$\left[\frac{Yb(III)}{Nd(III)}\right]_0$	$\left[\frac{Yb(III)}{Nd(III)}\right]_{eq}$	$\left[\frac{Yb(III)}{Nd(III)}\right]_{sorb.}$	$\alpha_{Yb/Nd}=\frac{\left[\frac{Yb(III)}{Nd(III)}\right]_{sorb.}}{\left[\frac{Yb(III)}{Nd(III)}\right]_{eq}}$
Alanine-based sorbent	0.922	0.767	1.45	1.89
Serine-based sorbent	0.922	0.792	1.68	2.12

4. Conclusions

Chitosan coated magnetic nano-based particles have been successfully modified by grafting alanine and serine (though epichlorohydrin crosslinking). These materials bind Nd(III) and Yb(III) at pH close to 5. The submicron size of sorbent particles limits the effect of the resistance to intraparticle diffusion and uptake kinetics are well fitted by the pseudo-second order rate equation. Sorption isotherms are modeled by the Langmuir equation and the maximum sorption capacities are relatively (around 10-20 mg metal g^{-1} depending on the sorbent and the metal). Taking into account the relative amount of magnetic core in the sorbent (i.e., ≈50%) the sorption capacity of chitosan derivative remains relatively how and the most significant advantage of these materials consists in the fast kinetics (equilibrium reached within approximately 3 hours) and the readily recovery of submicron-size of superparamagnetic materials by an external magnetic field. The study of sorption thermodynamics confirms the endothermic nature of the process (controlled by entropic rather than enthalpic effects). Metal ions can be successfully desorbed using acidic thiourea solution (0.5 M, pH 2.5-3), while the sorbents can be recycled for at least 4 cycles with a limited loss (<5%). in sorption efficiency. The separation factor $\alpha_{Yb/Nd}$ is close to 2: this means that the separation between heavy and light REES will be difficult (despite a preference of the sorbents for Yb(III) over Nd(III)).

Acknowledgments

This research was supported by the French Government through a fellowship granted from the French Embassy in Egypt (Institut Français d'Egypte). A special dedication is given to memory of Dr. Ahmed Donia.

References

Abdel-Rahman, A., A.H., El-Aassy, I.E.E., Fadia, Y.A. and Hamza, M.F. (2010), "Studies on the uptake of rare earth elements on polyacrylamidoxime resins from natural concentrate leachate solutions", *J. Dispersion Sci. Technol*., **31**(8), 1128-1135.

Donia, A.M., Atia, A.A. and Elwakeel, K.Z. (2007), "Recovery of gold(III) and silver(I) on a chemically modified chitosan with magnetic properties", *Hydrometallurgy*, **87**(3-4), 197-206.

Freundlich, H.M.F. (1906), "Uber die adsorption in lasungen", *Z. Phys. Chem*., **57**, 385-470.

Galhoum, A.A., Atia, A.A., Mahfouz, M.G., Abdel-Rehem, S.T., Gomaa, N.A., Vincent, T. and Guibal, E. (2015), "Dy(III) recovery from dilute solutions using magnetic-chitosan nano-based particles grafted with amino acids", *J. Mater. Sci*., **50**(7), 2832-2848.

Guibal, E. (2004), "Interactions of metal ions with chitosan-based sorbents: a review", *Sep. Purif. Technol*., **38**(1), 43-74.

Ho, Y.S. and McKay, G. (1999), "Pseudo-second order model for sorption processes", *Proc. Biochem*., **34**(5), 451-465.

Hosoba, M., Oshita, K., Katarina, R.K., Takayanagi, T., Oshima, M. and Motomizu, S. (2009), "Synthesis of novel chitosan resin possessing histidine moiety and its application to the determination of trace silver by ICP-AES coupled with triplet automated-pretreatment system", *Anal. Chim. Acta*, **639**(1-2), 51-56.

Hubicka, H. and Kolodynska, D. (2000), "Investigation into the use of macroporous anion exchangers for the sorption and separation of iminodiacetate complexes of lanthanum(III) and neodymium(III)", *Adsorpt. Sci. Technol*., **18**(8), 719-726.

Innocenzi, V., De Michelis, I., Kopacek, B. and Veglio, F. (2014), "Yttrium recovery from primary and secondary sources: A review of main hydrometallurgical processes", *Waste Manage. (Oxford)*, **34**(7), 1237-1250.

Khan, A., Badshah, S. and Airoldi, C. (2011), "Biosorption of some toxic metal ions by chitosan modified with glycidylmethacrylate and diethylenetriamine", *Chem. Eng. J.*, **171**(1), 159-166.

Lagergren, S. (1898), "About the theory of so-called adsorption of soluble substances", *Kungliga Svenska Vetenskapsakademiens*, **24**, 1-39.

Langmuir, I. (1918), "The adsorption of gases on plane surfaces of glass, mica and platinum", *J. Am. Chem. Soc*., **40**, 1361-1402.

Melnyk, I.V., Goncharyk, V.P., Kozhara, L.I., Yurchenko, G.R., Matkovsky, A.K., Zub, Y.L. and Alonso, B. (2012), "Sorption properties of porous spray-dried microspheres functionalized by phosphonic acid groups", *Microporous Mesoporous Mater*., **153**, 171-177.

Oshita, K., Takayanagi, T., Oshima, M. and Motomizu, S. (2007), "Adsorption behavior of cationic and anionic species on chitosan resins possessing amino acid moieties", *Anal. Sci*., **23**(12), 1431-1434.

Ren, Y., Abbood, H.A., He, F., Peng, H. and Huang, K. (2013), "Magnetic EDTA-modified chitosan/SiO2/Fe3O4 adsorbent: Preparation, characterization, and application in heavy metal adsorption", *Chem. Eng. J*., **226**, 300-311.

Roosen, J. and Binnemans, K. (2014), "Adsorption and chromatographic separation of rare earths with EDTA- and DTPA-functionalized chitosan biopolymers", *J. Mater. Chem. A*, **2**(5), 1530-1540.

Ruiz, M., Sastre, A.M. and Guibal, E. (2002a), "Pd and Pt recovery using chitosan gel beads: II. Influence of chemical and physical modification on sorption properties", *Sep. Sci. Technol*., **37**(10), 2385-2403.

Ruiz, M.A., Sastre, A.M. and Guibal, E. (2002b), "Pd and Pt recovery using chitosan gel beads: I. Influence of drying process on diffusion properties", *Sep. Sci. Technol*., **37**(9), 2143-2166.

Sun, X., Ji, Y., Chen, J. and Ma, J. (2009), "Solvent impregnated resin prepared using task-specific ionic liquids for rare earth separation", *J. Rare Earths*, **27**(6), 932-936.

Texier, A.C., Andres, Y. and Le Cloirec, P. (1999), "Selective biosorption of lanthanide (La, Eu, Yb) ions by Pseudomonas aeruginosa", *Environ. Sci. Technol*., **33**(3), 489-495.

Tien, C. (1994), Adsorption Calculations and Modeling, Butterworth-Heinemann, Newton, MA.

Vander Hoogerstraete, T. and Binnemans, K. (2014), "Highly efficient separation of rare earths from nickel and cobalt by solvent extraction with the ionic liquid trihexyl(tetradecyl) phosphonium nitrate: a process relevant to the recycling of rare earths from permanent magnets and nickel metal hydride batteries", *Green Chem.*, **16**(3), 1594-1606.

Vijayaraghavan, K., Sathishkumar, M. and Balasubramanian, R. (2011), "Interaction of rare earth elements with a brown marine alga in multi-component solutions", *Desalination*, **265**(1-3), 54-59.

Vlachou, A., Symeopoulos, B.D. and Koutinas, A.A. (2009), "A comparative study of neodymium sorption by yeast cells", *Radiochim. Acta*, **97**(8), 437-441.

Wang, Z.H., Ma, G.X., Lu, J., Liao, W.P. and Li, D.Q. (2002), "Separation of heavy rare earth elements with extraction resin containing 1-hexyl-4-ethyloctyl isopropylphosphonic acid", *Hydrometallurgy*, **66**(1-3), 95-99.

Weber, W.J. and Morris, J.C. (1963), "Kinetics of adsorption on carbon from solutions", *J. Sanit. Eng. Div*., ASCE, **89**(2), 31-60.

Wu, D., Zhang, L., Wang, L., Zhu, B. and Fan, L. (2011), "Adsorption of lanthanum by magnetic alginate-chitosan gel beads", *J. Chem. Technol. Biotechnol*., **86**(3), 345-352.

Xie, F., Zhang, T.A., Dreisinger, D. and Doyle, F. (2014), "A critical review on solvent extraction of rare earths from aqueous solutions", *Miner. Eng*., **56**, 10-28.

Xiong, C., He, R., Pi, L., Li, J., Yao, C., Jiang, J. and Zheng, X. (2015), "Adsorption of neodymium(III) on acrylic resin (110 resin) from aqueous solutions", *Sep. Sci. Technol*., **50**(4), 564-572.

Xiong, C., Yao, C. and Wang, Y. (2006), "Sorption behaviour and mechanism of ytterbium(III) on imino-diacetic acid resin", *Hydrometallurgy*, **82**(3-4), 190-194.

Xu, J., Chen, M., Zhang, C. and Yi, Z. (2013), "Adsorption of uranium(VI) from aqueous solution by diethylenetriamine-functionalized magnetic chitosan", *J. Radioanal. Nucl. Chem*., **298**(2), 1375-1383.

Xu, T. and Peng, H. (2009), "Formation cause, composition analysis and comprehensive utilization of rare earth solid wastes", *J. Rare Earths*, **27**(6), 1096-1102.
Yang, G., Tang, L., Lei, X., Zeng, G., Cai, Y., Wei, X., Zhou, Y., Li, S., Fang, Y. and Zhang, Y. (2014), "Cd(II) removal from aqueous solution by adsorption on α-ketoglutaric acid-modified magnetic chitosan", *Appl. Surf. Sci*., **292**, 710-716.
Zeldowitsch, J. (1934), "The catalytic oxidation of carbon monoxide on manganese dioxide", *Acta Physicochimica URSS*, **1**, 364-449.
Zhang, W., Ye, G. and Chen, J. (2012), "TRPO impregnated Levextrel resin: Synthesis and extraction behavior of Zr (IV) and Nd (III) ions", *Sep. Sci. Technol*., **48**(2), 263-271.
Zheng, Z. and Xiong, C. (2011), "Adsorption behavior of ytterbium (III) on gel-type weak acid resin", *J. Rare Earths*, **29**(5), 407-412.
Zhou, L., Liu, Z., Liu, J. and Huang, Q. (2010), "Adsorption of Hg(II) from aqueous solution by ethylenediamine-modified magnetic crosslinking chitosan microspheres", *Desalination*, **258**(1-3), 41-47.
Zhou, Z., Lin, S., Yue, T. and Lee, T.-C. (2014), "Adsorption of food dyes from aqueous solution by glutaraldehyde cross-linked magnetic chitosan nanoparticles", *J. Food Eng*., **126**, 133-141.

WL

Appendix

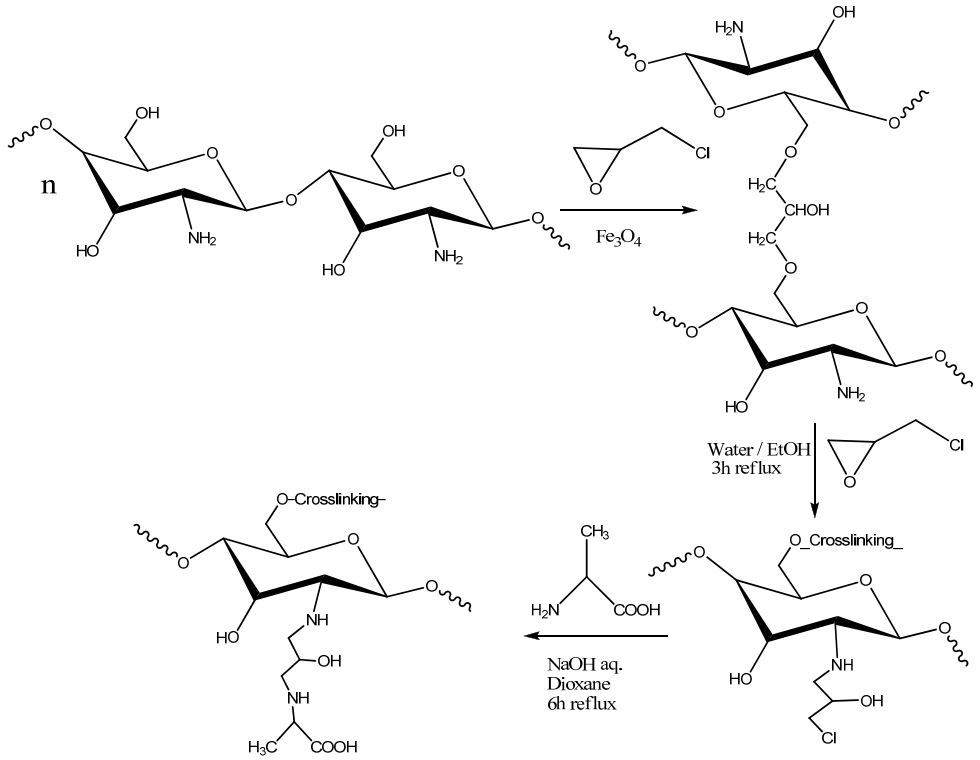

Fig. AM1 Scheme for the synthesis of alanine functionalized chitosan magnetic nano-based particles

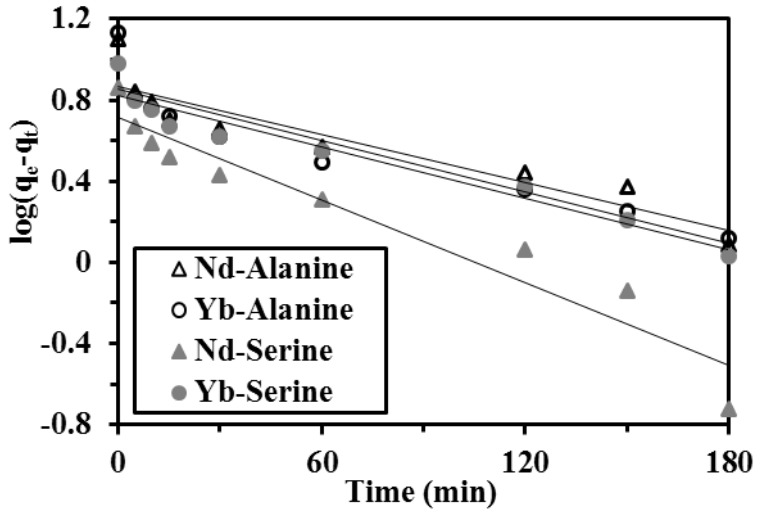

Fig. AM2 Fitting of uptake kinetics with the PFORE for Nd(III) and Yb(III) recovery using alanine and serine functionalized chitosan magnetic nano-based particles (data from Fig. 3)

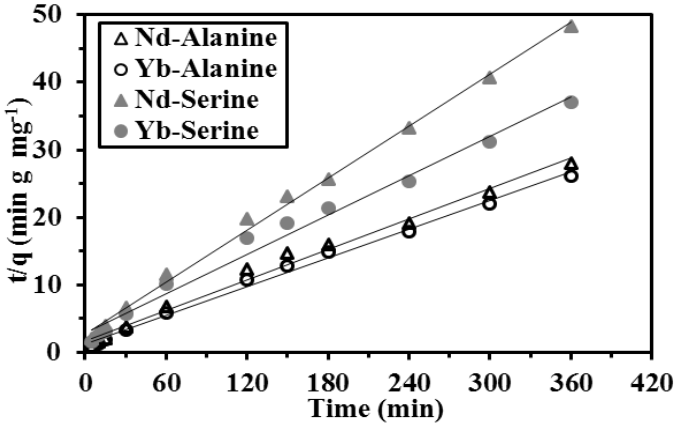

Fig. AM3 Fitting of uptake kinetics with the PSORE for Nd(III) and Yb(III) recovery using alanine and serine functionalized chitosan magnetic nano-based particles (data from Fig. 3)

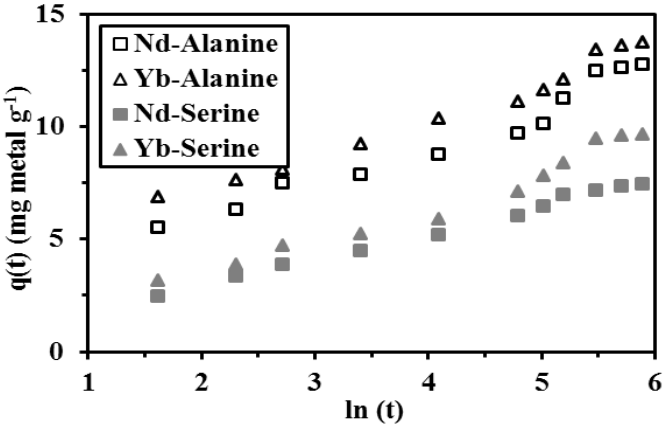

Fig. AM4 Fitting of uptake kinetics with the Elovich equation for Nd(III) and Yb(III) recovery using alanine and serine functionalized chitosan magnetic nano-based particles (data from Fig. 3)

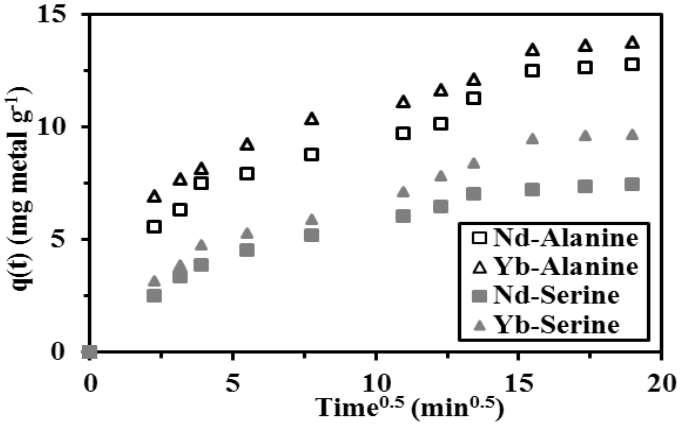

Fig. AM5 Fitting of uptake kinetics with the sRIDE equation for Nd(III) and Yb(III) recovery using alanine and serine functionalized chitosan magnetic nano-based particles (data from Fig. 3)